

## Peculiarities of Nuclear Fusion in Synthesis of Superheavy Elements

A. K. Nasirov,<sup>\*,a,b</sup> G. Giardina,<sup>c</sup> A. I. Muminov,<sup>b</sup> G. Mandaglio,<sup>c</sup> and R. K. Utamuratov<sup>a,b</sup>

<sup>a</sup>Joint Institute for Nuclear Research, Dubna, 141980, Moscow region, Russia

<sup>b</sup>Heavy Ion Physics Department, Institute of Nuclear Physics, 100214, Tashkent, Uzbekistan

<sup>c</sup>INFN, Sezione di Catania, and Dipartimento di Fisica dell'Università di Messina, 98166, Messina, Italy

Received: December 20, 2006; In Final Form: April 23, 2007

The role of entrance channel for reactions with massive nuclei is discussed by comparison of experimental data of reactions with different mass (charge) asymmetry and leading to different isotopes of the superheavy element  $Z = 112$ . Three stages (capture, complete fusion, and formation of evaporation residues) of the so called “cold” and “hot” fusion reactions are considered for  $^{70}\text{Zn} + ^{208}\text{Pb}$  and  $^{48}\text{Ca} + ^{238}\text{U}$  reactions which were used to synthesize superheavy elements  $Z = 112$ . It is shown that the collisions by the orientation angles  $30^\circ < \alpha_p < 60^\circ$  for projectile and  $30^\circ < \alpha_r < 45^\circ$  for the target nucleus lead to the largest cross section in synthesis of superheavy element in the  $^{48}\text{Ca} + ^{238}\text{U}$  reaction at  $E_{\text{CN}}^* = 35$  MeV.

### 1. Introduction

The small probabilities of synthesis of new superheavy elements at GSI (Darmstadt, Germany), Joint Institute for Nuclear Research (Dubna, Russia), and RIKEN (Wako, Japan) during the last decade stimulate the experimental and theoretical studies of the nuclear reaction mechanism.<sup>1-4</sup> In preparation of these experiments, the main aim is to reach maximum cross sections of the yield of evaporation residues (ER) as a result of the de-excitation of the heated compound nucleus which is formed in complete fusion of the projectile and target nuclei. Because the ER excitation function in the synthesis of superheavy elements has very narrow width for “cold fusion” reactions (5–10 MeV) with  $^{208}\text{Pb}$  and  $^{209}\text{Bi}$  targets<sup>5</sup> and the width of the “hot fusion” reactions with  $^{48}\text{Ca}$  projectile on actinide targets<sup>6</sup> is more wider (15–20 MeV). It is interesting to compare “hot” ( $E_{\text{CN}}^* > 30$  MeV) and “cold” ( $E_{\text{CN}}^* < 25$  MeV) fusion reactions. In the “hot fusion”  $^{30}\text{Si} + ^{238}\text{U}$  reaction, sufficiently low ER cross section 70 pb for the synthesis of superheavy element  $^{263}\text{Sg}$  in 5n-channel was observed while the isotope  $^{260}\text{Sg}$  was obtained with large cross section 2500 pb in the “cold fusion”  $^{54}\text{Cr} + ^{208}\text{Pb}$  reaction. The smallness of the ER cross section in the “hot fusion”  $^{30}\text{Si} + ^{238}\text{U}$  reactions is explained by the small survival probability of the compound nucleus with the excitation energy 50 MeV at de-excitation of 5 neutrons.<sup>1,2</sup> The use of the  $^{48}\text{Ca}$  beam leads to the relatively high cross section of the evaporation residues due to large binding energy of  $^{48}\text{Ca}$ . Therefore, the maximum of cross section of the yield of superheavy elements corresponds to 35 MeV while in the “hot fusion” reactions the maximum value of evaporation residues yield is observed at 50 MeV.<sup>7-9</sup>

So, for experiments it is important to know the favorable range of beam energy before experiments. The use of the “cold fusion” reactions with projectiles  $^{50}\text{Ti}$ ,  $^{54}\text{Cr}$ ,  $^{56}\text{Fe}$ ,  $^{64}\text{Ni}$ , and  $^{70}\text{Zn}$  on the  $^{208}\text{Pb}$  and  $^{209}\text{Bi}$  targets succeeded in synthesizing superheavy elements  $Z = 102, 104, 106, 108, 110, 111,$  and  $112$  in GSI while the use of  $^{48}\text{Ca}$  projectile and actinide targets allows one to synthesize more heavy superheavy elements  $Z = 114, 115, 116,$  and  $118$  in JINR. The last experiments of “cold fusion” reactions were performed in RIKEN where the new element  $Z = 113$  was observed in the  $^{70}\text{Zn} + ^{209}\text{Bi}$  reaction.<sup>10</sup>  $Z$

$= 113$  seems to be a heaviest superheavy element which was obtained in “cold fusion” reaction due to drastic decrease of fusion probability with increase of the projectile charge number in reactions with  $^{208}\text{Pb}$  and  $^{209}\text{Bi}$  targets.

The way to obtain nucleus as possible less excited seems to be preferable but in this case amount of formed compound nuclei may be very small due to a hindrance at its formation, i.e., very small complete fusion cross section. As a result yield of superheavy elements will be extremely small to be observed. Therefore, it is important to increase fusion cross section by increase of the beam energy. But the survival probability of a hot compound nucleus should not decrease so much by increase of excitation energy to avoid decreasing of the yield of ER. Note we should avoid the large values of compound nucleus angular momentum ( $\ell$ ) which decreases strongly its survival probability. The actinide nuclei are mainly prolate deformed. The distribution in the space of the orientation angles of their axial symmetry axis  $\alpha$  to the beam direction is arbitrary. The dependence of the complete fusion probability on  $\alpha$  allows us to calculate the beam energy providing a large partial fusion cross section with small angular momentum of compound nucleus. In this work we will analyse the role played by shell structure and orientation angles of the symmetry axis of colliding nuclei in formation of ER.

The rotated dinuclear system (DNS) is formed as intermediate stage in deep-inelastic collisions, quasifission, complete fusion, and fast-fission reactions with the different lifetime. The complete fusion of nuclei occurs through the stage of formation of DNS which can evolve to the hot compound nucleus in competition with breaking up after the intense nucleon transfer between its constituents (quasifission). In reactions with massive nuclei, the contributions of the quasifission fragments are dominate in comparison with ones of fusion-fission mechanism. The mass distribution of the quasifission fragments can have different shapes including the symmetric shape of fusion-fission reaction fragments as a function of the beam energy, initial mass asymmetry, and shell structure of reacting nuclei. In the analysis of experimental data there are difficulties in separation of fragments according to their origination to estimate the experimental cross sections of different mechanisms. It is important to study all three stages of reaction with massive nuclei in synthesis of superheavy elements to determine the optimal beam energy providing as possible larger values of the ER cross sections.

\*Corresponding author. E-mail: nasirov@jinr.ru. Fax: +7-49621-65084.

**TABLE 1: Comparison of the main characteristics of the “cold” and “hot” fusion in case of the  $^{70}\text{Zn} + ^{208}\text{Pb}$  and  $^{48}\text{Ca} + ^{238}\text{U}$  reactions used to synthesize superheavy element  $Z = 112$**

	$^{70}\text{Zn} + ^{208}\text{Pb}$	$^{48}\text{Ca} + ^{238}\text{U}$
Compound nucleus	$^{278}122$	$^{286}112$
$\delta W / \text{MeV}$	-5.08	-5.94
$S_n / \text{MeV}$	7.14	6.95
$E_{\text{CN}}^* / \text{MeV}$	12	35
$\sigma_{\text{ER}}^{\text{exp}} / \text{pb}$	$0.5^{+1.1}_{-0.5}$ (Reference 5)	$2.5^{+1.8}_{-1.5}$ (Reference 6)
$\sigma_{\text{ER}}^{\text{theor}} / \text{pb}$	0.7 (Reference 11)	5.2 (Reference 12)
$\sigma_{\text{fus}} / \text{nb}$	0.3	50
$\sigma_{\text{cap}} / \text{mb}$	2.5	40

$\delta W$ : shell corrections to binding energy of compound nucleus.  $S_n$ : neutron separation energy.  $E_{\text{CN}}^*$ : excitation energy of compound nucleus.  $\sigma_{\text{ER}}$ : maximum values of the evaporation residue cross section.  $\sigma_{\text{fus}}$  and  $\sigma_{\text{cap}}$ : theoretical complete fusion and capture cross sections, respectively.

## 2. Three Stages of the Evaporation Residues Formation

The three stages are: (a) capture of projectile-nucleus by nucleus of target and formation of the molecular-like dinuclear system, (b) complete fusion which is transformation of the dinuclear system into a hot compound nucleus in competition with the quasifission process, and (c) formation of the ER after emission of neutrons and charged particles from the heated compound nucleus in competition against fission. The experiments of synthesis of superheavy elements in the Flerov Laboratory of Nuclear Reaction showed that to synthesize the element  $Z = 112$  the “hot fusion”  $^{48}\text{Ca} + ^{238}\text{U}$  reaction<sup>6</sup> is more preferable than so called “cold fusion”  $^{70}\text{Zn} + ^{208}\text{Pb}$  reaction.<sup>5</sup> It is seen in comparison of the measured cross sections for the ER for these reactions presented in Table 1. Theoretical results<sup>11,12</sup> obtained in description of this experimental data allows us to estimate the dependence of the synthesis probability of  $Z = 112$  element on each stage of the reaction mechanism, for example, capture and fusion cross sections,  $\sigma_{\text{cap}}$  and  $\sigma_{\text{fus}}$ , respectively. Their maximal values are presented in Table 1. The advantage of the “hot fusion” reaction in comparison with “cold fusion” at synthesis of the superheavy element  $Z = 112$  seems to be clear according to experimental data. It is explained by the calculated larger values of capture  $\sigma_{\text{cap}}$  and fusion  $\sigma_{\text{fus}}$  cross sections for the  $^{48}\text{Ca} + ^{238}\text{U}$  reaction in comparison with that for the  $^{70}\text{Zn} + ^{208}\text{Pb}$  reaction (Table 1). The shell corrections to binding energy of compound nucleus  $^{286}112$  is larger by 0.9 MeV in comparison with one of  $^{278}112$ . The neutron separation energies of the formed compound nuclei are comparable. But the surviving probability of the compound nucleus  $^{286}112$  formed in the former reaction is smaller than that of the compound nucleus  $^{278}112$  formed in the  $^{70}\text{Zn} + ^{208}\text{Pb}$  reaction due to large excitation energy  $E_{\text{CN}}^*$ . The main factor which provides the observable cross section of the ER is the large fusion probability of nuclei in the  $^{48}\text{Ca} + ^{238}\text{U}$  reaction. In Figure 1, we compare the experimental and calculated cross sections of capture, complete fusion, and formation of ER after neutron emission from the compound nucleus for the  $^{48}\text{Ca} + ^{238}\text{U}$  reaction. The capture cross section is, qualitatively, in good agreement with experimental data whereas the calculated fusion cross section is much smaller than the extracted values for fusion from the measured data of reaction fragments. It seems to us that the experimental data for fission fragments can contain a contribution of the quasifission fragments which are

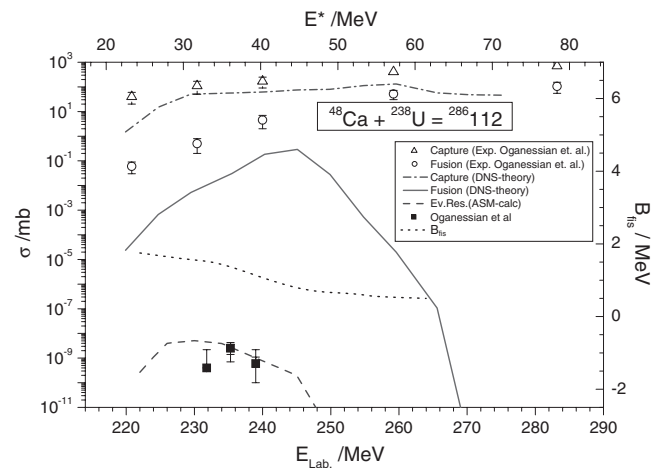


**Figure 1.** Comparison of the experimental<sup>6</sup> (symbols) and calculated<sup>12</sup> (lines) excitation functions of capture, complete fusion, and formation of evaporation residues after neutron emission from the excited compound nucleus for the  $^{48}\text{Ca} + ^{238}\text{U}$  reaction (left axis). Fission barrier of the excited and rotated compound nucleus as a function of beam energy (right axis) is also shown.

formed without formation of compound nucleus but their mass distribution may have a shape of the one of fission fragments. Unfortunately, in analysis of the experimental data, it is difficult to separate the pure fusion-fission fragments from the fragments of quasifission. Due to full momentum transfer in both reactions their fragments have similar total kinetic energy distribution. As a function of the initial orbital angular momentum and beam energy of the projectile the mass distribution of the quasifission fragments can be overlapped with the one of fusion-fission fragments. In these experiments the angular distribution was not measured and, therefore, there is an ambiguity in extraction of fusion cross section from the measured binary fragments of full momentum reactions. Theoretical calculations are not free from some assumptions and free parameters as a radius parameters  $r_0$ . Therefore, the exact ratio of contributions of quasifission and complete fusion fragments into measured data is still questionable.

In Figure 1, the fission barrier of the heated compound nucleus is also presented as a function of excitation energy. The cross sections of evaporation residues formation are described well by use of the advanced statistical model. In this model, the damping of the nuclear shell correction by increase of angular momentum of compound nucleus is taken into account. The spin distribution of compound nucleus plays the decisive role in calculation of survival probability. It is formed by the partial fusion cross sections which are determined by the features of potential energy surface<sup>13,14</sup> of DNS and friction coefficients (radial, tangential)<sup>15</sup> for the given value of the beam energy and initial orbital angular momentum  $L_0$ . Note the potential energy surface is a function of the orientation angles of the axial symmetry axis of reacting nuclei.<sup>16</sup> The small cross section at synthesis of the  $^{277}112$  element in the  $^{70}\text{Zn} + ^{208}\text{Pb}$  reaction is explained by the large hindrance for complete fusion (see Figure 2) in “cold fusion” reactions. The strong hindrance to fusion is connected with the location of the initial charge asymmetry of this reaction in the valley corresponding to the magic nucleus  $^{208}\text{Pb}$  which is seen in Figure 5. In the next section we will compare the capture and fusion cross sections for reactions under discussion.

**2.1. Peculiarities of capture and fusion in hot and cold fusion reactions.** In our model (see References 13 and 14), the capture occurs if the heavy-ion collision path is in the potential well after overcoming of the Coulomb barrier and dissipation of the main part of the relative kinetic energy. In the deep inelastic collisions projectile or projectile-like fragment over-

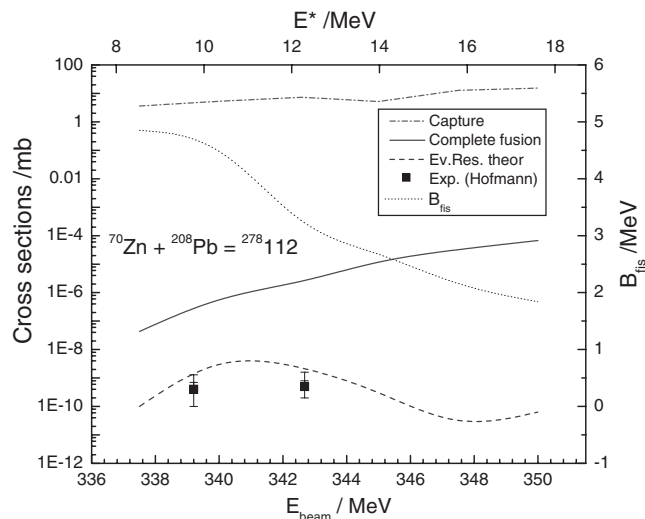


**Figure 2.** Comparison of the experimental data of the evaporation residues<sup>5</sup> (symbols) and calculated<sup>11</sup> (lines) excitation functions of capture, complete fusion, and formation of evaporation residues after neutron emission from the excited compound nucleus for the  $^{70}\text{Zn} + ^{208}\text{Pb} = ^{278}112$  reaction (left axis). Fission barrier of the excited and rotated compound nucleus as a function of beam energy (right axis).

comes the Coulomb barrier from inner part to outside (exit channel) due to the smallness of dissipation of kinetic energy (see figure 1 in Reference 11). It is clear that deep inelastic collision occurs at higher energies of projectile above the Coulomb barrier than in the case of capture for a given value of the orbital angular momentum, because the friction coefficient is not strong to trap all trajectories into potential well.<sup>16</sup> The amount of energy above the Coulomb barrier determines which of these two processes occurs. If capture occurs, then we calculate the competition between quasifission and complete fusion. In collision of deformed nuclei with different orientations proportion between contributions of deep inelastic collisions and capture, as well as proportion between quasifission and complete fusion are different at the same beam energy and orbital angular momentum. To reach an agreement with the experimental data for capture cross section we take into account the deformation parameters connected to the  $2^+$  and  $3^-$  collective excitations in the spherical nuclei. It was done by use of the mean-square values of the deformation parameters<sup>17,18</sup> corresponded to above mentioned excitations. The partial fusion cross-sections, which are used to calculate the ER cross-section along the de-excitation cascade of compound nucleus, are obtained by averaging over all orientations (in detail see Reference 16). Analysis of the dependence of the partial cross sections of complete fusion on the orientation angles of colliding nuclei showed that large fusion probability with the small values of compound nucleus angular momentum is observed in the range  $30^\circ$ – $60^\circ$  for the orientation angles of symmetry axis for projectile and  $60^\circ$ – $75^\circ$  for ones of the target nucleus. Some examples are shown in Figure 3 for the  $^{48}\text{Ca} + ^{238}\text{U}$  reaction. So the large fusion probability is obtained at the small values of angular momentum in heavy ion collisions when orientation angles of the projectile and target symmetry axis are in the corresponding above mentioned ranges. This case is shown on the right top panel of Figure 3. It is seen that partial fusion cross section is small for the around tip–tip ( $0^\circ$ – $0^\circ$ ) and side–side ( $90^\circ$ – $90^\circ$ ) orientations. In the former case quasifission is a dominate channel while in the latter case capture cross section is small due to shallow potential well. It is seen from Figure 4. The maximum cross sections corresponds to those values of beam energy at which the three events of synthesis of superheavy element  $Z = 112$  was observed in the Flerov Laboratory of Nuclear Reactions (see Figure 1). We

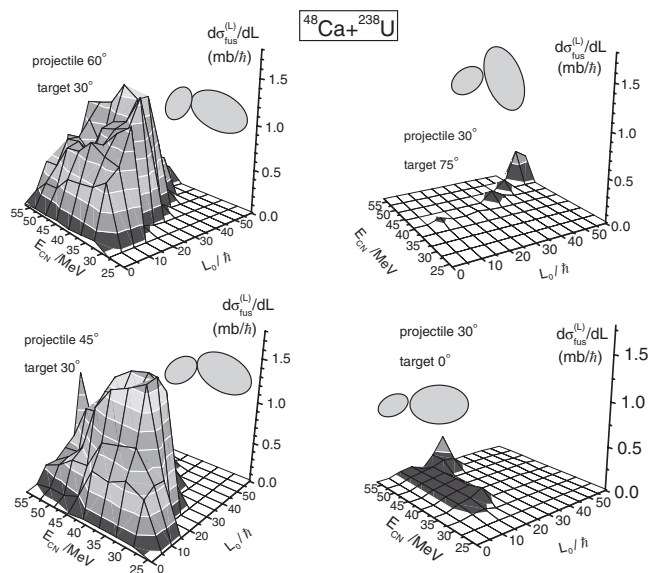


**Figure 3.** Dependence of the partial fusion cross sections on the orientation angles of symmetry axis of colliding nuclei ( $\beta_2(^{238}\text{U}) = 0.21$ ;  $\beta_2(2^+ \text{-excitation } ^{48}\text{Ca}) = 0.1$  from Reference 17) as a function of the initial orbital angular momentum  $L_0$  and excitation energy of compound nucleus  $E_{CN}$ .

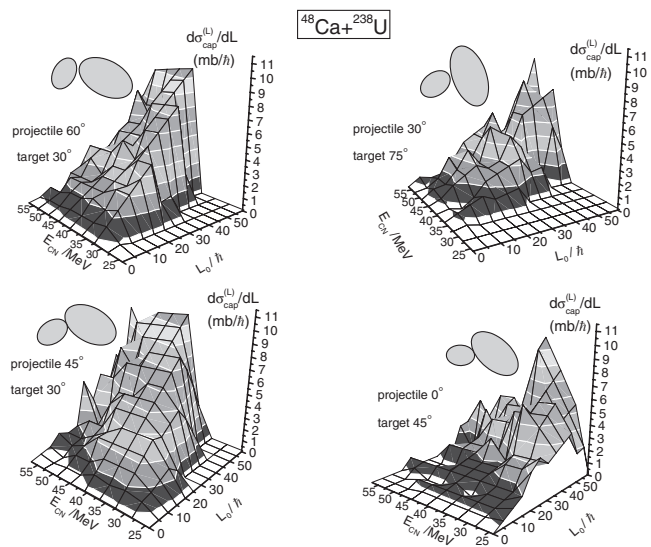


**Figure 4.** Same as in Figure 3 but for the partial capture cross sections.

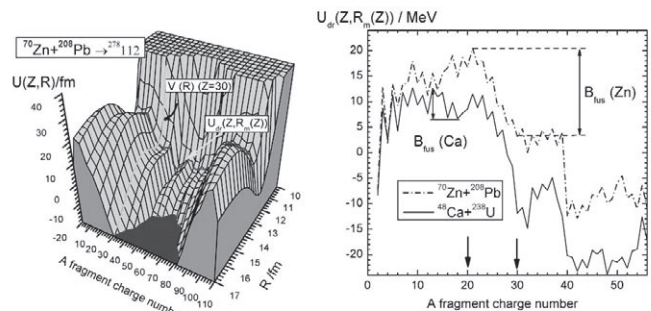


**Figure 5.** Potential energy surface (left panel) and driving potential (right panel) for the cold and hot fusion reactions leading to  $Z = 112$ . The nucleus–nucleus potential ( $\ell = 0$ ) for the  $^{70}\text{Zn} + ^{208}\text{Pb}$  reaction and driving potential for the dinuclear system are shown by arrows. Intrinsic fusion barrier ( $B_{fus}^*(\text{Zn})$ ) for the “cold” fusion is sufficiently larger than the one ( $B_{fus}^*(\text{Ca})$ ) for the “hot” fusion reaction.

came to our conclusion that this beam energy value  $E_{\text{lab}} = 235$  MeV is favorable to observe the largest cross section of evaporation residues due to relatively large values of the partial fusion cross section with small angular momentum ( $L < 25 \hbar$ ) of compound nucleus is obtained.

We calculate the cross section of ER formed after each step  $x$  of the de-excitation cascade after the emission from the hot CN of particles  $\nu(x)n + y(x)p + k(x)\alpha + s(x)$  (where  $\nu$ ,  $y$ ,  $k$ , and  $s$  are numbers of neutrons, protons,  $\alpha$ -particles, and  $\gamma$ -quanta) by formula

$$\sigma_{\text{ER}}^{(x)}(E_{\text{c.m.}}) = \sum_{\ell=0}^{\ell_d} (2\ell+1) \sigma_{\ell}^{(x-1)}(E_{\text{c.m.}}) W_{\text{sur}}^{(x-1)}(E_{\text{c.m.}} + Q_{\text{gg}}, \ell), \quad (1)$$

where  $\sigma_{\ell}^{(x-1)}(E_{\text{c.m.}}, \ell)$  is the partial formation cross section of the excited intermediate nucleus of the  $(x-1)$ th step and  $W_{\text{sur}}^{(x-1)}(E_{\text{c.m.}} + Q_{\text{gg}}, \ell)$  is the survival probability of the  $(x-1)$ th intermediate nucleus against fission along the de-excitation cascade of CN. It is clear that  $\sigma_{\ell}^{(0)}(E_{\text{c.m.}}, \ell) = \sigma_{\ell}^{(\text{fus})}(E_{\text{c.m.}}, \ell)$ . Our method of calculation (also including the advanced statistical method<sup>19,20</sup>) of the ER cross sections takes into account the damping of the shell correction in the fission barrier as a function of the excitation energy and orbital angular momentum. This is accounted for the various steps of the de-excitation cascade of the compound nucleus leading to the fission fragments or the ER nuclei in the exit channel.<sup>13,14,21</sup>

The fusion cross section is related to the number of events corresponding to the transformation of the dinuclear system into compound nucleus in competition with the quasi-fission process. It is defined by the product of the partial capture cross section and the related fusion factor  $P_{\text{CN}}$  which allows to take into account the competition between the complete fusion and quasifission processes:

$$\sigma_{\text{fus}}^{(\ell)}(E_{\text{c.m.}}) = \sigma_{\text{capture}}^{(\ell)}(E_{\text{c.m.}}) P_{\text{CN}}(E_{\text{c.m.}}, \ell). \quad (2)$$

The capture cross section is calculated by solution of the dynamical equations of motion for radial distance and orbital angular momentum (details see in References 13, 14, and 16). Calculations showed that a ‘‘window’’ of the  $\ell$  values leading to capture may appear. For example, there is no capture with the values  $\ell < 30$  of angular momentum at  $E_{\text{lab}} > 225$  MeV ( $E_{\text{CN}} = 28.1$  MeV) for the small orientation angles of target and projectile symmetry axis as shown in the right bottom panel of Figure 4.

During the formation of the dinuclear system at the capture stage there is an intense nucleon exchange between reacting nuclei. In the quasifission and fusion processes, an intense mass transfer takes place and, in depending on the entrance channel, the mass asymmetry degree of freedom may be fully or partially equilibrated.<sup>22</sup> As a result, while DNS exists, we have an ensemble  $\{Z\}$  of the DNS configurations which contribute to the competition between complete fusion and quasifission with the probabilities  $\{Y_Z\}$ . Position of the maximum of the mass distribution is determined by the peculiarities of the nuclear shell structure and lifetime of the dinuclear system.<sup>16</sup> Therefore, the statistical calculation of  $P_{\text{CN}}(E_{\text{DNS}}^*, \ell)$  is performed by the formula:

$$P_{\text{CN}}(E_{\text{DNS}}^*, \ell) = \sum_{Z=Z_{\text{sym}}}^{Z_{\text{max}}} Y_Z(E_{\text{DNS}}^*, \ell) P_{\text{CN}}^{(Z)}(E_{\text{DNS}}^*, \ell), \quad (3)$$

where  $Y_Z(E_{\text{DNS}}^*, \ell)$  is the probability of population of the DNS configuration  $(Z, Z_{\text{tot}} - Z)$  at  $E_{\text{DNS}}^*(Z)$  and  $\ell$ ;  $Z_{\text{sym}} = (Z_1 + Z_2)/2$ ;  $Z_{\text{max}}$  corresponds to the charge asymmetry where the driving potential reaches its maximum ( $B_{\text{fus}}^*(Z_{\text{max}}) = 0$ ) (see References 13 and 14);

$$P_{\text{CN}}^{(Z)}(E_{\text{DNS}}^*, \ell) = \frac{\rho(E_{\text{DNS}}^*(Z) - B_{\text{fus}}^*(Z, \ell))}{\rho(E_{\text{DNS}}^*(Z) - B_{\text{fus}}^*(Z, \ell)) + \rho(E_{\text{DNS}}^*(Z) - B_{\text{qf}}(Z, \ell))}, \quad (4)$$

where the intrinsic fusion barrier  $B_{\text{fus}}^*(Z, \ell)$  being a function of the charge asymmetry and angular momentum of DNS is found from the driving potential<sup>13,14,16</sup> (see Figure 5). The quasifission barrier  $B_{\text{qf}}(Z, \ell)$  for the considered fragment depends on its charge number and is determined by the depth of potential well of the nucleus-nucleus interaction of the DNS fragment with its partner nucleus. Therefore, transformation of the DNS into compound nucleus by complete fusion is a function of the charge asymmetry of the DNS constituents.

In eq 4,  $\rho(E_{\text{DNS}}^*(Z) - B_{\text{fus}}^*(Z, \ell))$  is the DNS level density calculated on the quasifission and intrinsic fusion barriers ( $B_{\text{K}} = B_{\text{qf}}, B_{\text{fus}}^*$ ). For more details see Reference 16.

Both characteristics of the fusion excitation function, namely, its maximum value and width (energy window for the complete fusion) are related to the ratio between  $B_{\text{fus}}^*$  and  $B_{\text{qf}}$  for the given reaction.

### 3. Conclusion

Hot fusion reactions with the  $^{48}\text{Ca}$ -projectile can be successfully used in synthesis of superheavy elements due to reducing of excitation energy of compound nucleus up to 35–40 MeV. The loss of events by high intensity of fission should be compensated by large fusion cross section in comparison with  $^{70}\text{Zn} + ^{208}\text{Pb}$  reaction. Advantage of the use of the double magic  $^{48}\text{Ca}$  projectile allowed us to decrease of 15 MeV excitation energy of compound nucleus in synthesis of superheavy elements up to  $Z = 118$ . The observable values of the evaporation residues is provided by the large partial fusion cross section at as possible as low excitation energy and angular momentum of compound nucleus.

In our calculations,  $E_{\text{CN}}^* = 35$  MeV corresponds to the beam energy which is 5–10 MeV higher than interaction barriers at the projectile orientation angles  $30^\circ < \alpha_p < 60^\circ$  and that  $30^\circ < \alpha_t < 45^\circ$  for the target nucleus. These angles are taken relative to the beam direction. In case of the  $^{30}\text{Si} + ^{238}\text{U}$  reaction,  $E_{\text{CN}}^* = 50$  MeV corresponds to the similar intermediate orientation angles. The equatorial collisions make relatively small contributions in comparison with the above mentioned angles.

**Acknowledgement.** One of authors (A.K.N.) thanks Drs. Y. Aritomo, K. Hagino, H. Ikezoe, A. Iwamoto, K. Morita, K. Nishio, M. Ohta, T. Ohtsuki, N. Tagikawa, W. Scheid, V. V. Volkov, and T. Wada for fruitful discussions and he is grateful to the Japan Society for the Promotion Science for support his research in collaboration with scientists of Japan Atomic Energy Agency and to Drs. Katsuhisa Nishio and Yoshihiro Aritomo, as well as Japanese colleagues in the Advanced Science Research Center of JAEA, RIKEN, and Konan and Tohoku Universities for warm hospitality.

### References

- (1) K. Nishio, S. Hofmann, F. P. Heßberger, D. Ackermann, S. Antalic, V. F. Comas, Z. Gan, S. Heinz, J. A. Heredia, H. Ikezoe, J. Khuyagbaatar, B. Kindler, I. Kojouharov, P. Kuusiniemi, B. Lommel, R. Mann, M. Mazzocco, S. Mitsuoka, Y. Nagame, T. Ohtsuki, A. G. Popeko, S. Saro, H. J. Schött, B. Sulignano, A. Svirikhin, K. Tsukada, K. Tsuruta, and A. V. Yeremin, *Eur. Phys. J. A* **29**, 281 (2006).
- (2) K. E. Gregorich, *Phys. Rev. C* **74**, 044611 (2006).
- (3) G. G. Adamian, N. V. Antonenko, and W. Scheid, *Phys. Rev. C* **69**, 044601 (2004).
- (4) Y. Aritomo, *Nucl. Phys. A* **780**, 222 (2006).

- (5) S. Hofmann and G. Münzenberg, *Rev. Mod. Phys.* **72**, 733 (2000).
- (6) Yu. Ts. Oganessian, V. K. Utyonkov, Yu. V. Lobanov, F. Sh. Abdullin, A. N. Polyakov, I. V. Shirokovsky, Yu. S. Tsyganov, G. G. Gulbekian, S. L. Bogomolov, B. N. Gikal, A. N. Mezentsev, S. Iliev, V. G. Subbotin, A. M. Sukhov, A. A. Voinov, G. V. Buklanov, K. Subotic, V. I. Zagrebaev, M. G. Itkis, J. B. Patin, K. J. Moody, J. F. Wild, M. A. Stoyer, N. J. Stoyer, D. A. Shaughnessy, J. M. Kenneally, P. A. Wilk, R. W. Lougheed, R. I. Il'kaev, and S. P. Vesnovskii, *Phys. Rev. C* **70**, 064609 (2004).
- (7) A. N. Andreyev, D. D. Bogdanov, V. I. Chepigin, A. P. Kabachenko, O. N. Malyshev, Yu. Ts. Oganessian, R. N. Sagajdak, G. M. Ter-Akopian, A. V. Yeremin, F. P. Hessberger, S. Hofmann, V. Ninov, M. Florek, S. Saro, and M. Veselsky, *Z. Phys. A* **344**, 225 (1992).
- (8) Yu. A. Lazarev, Yu. V. Lobanov, Yu. Ts. Oganessian, Yu. S. Tsyganov, V. K. Utyonkov, F. Sh. Abdullin, S. Iliev, A. N. Polyakov, J. Rigol, I. V. Shirokovsky, V. G. Subbotin, A. M. Sukhov, G. V. Buklanov, B. N. Gikal, V. B. Kutner, A. N. Mezentsev, I. M. Sedykh, D. V. Vakarov, R. W. Lougheed, J. F. Wild, K. J. Moody, and E. K. Hulet, *Phys. Rev. Lett.* **75**, 1903 (1995).
- (9) K. E. Gregorich, W. Loveland, D. Peterson, P. M. Zielinski, S. L. Nelson, Y. H. Chung, Ch. E. Düllmann, C. M. Folden III, K. Aleklett, R. Eichler, D. C. Hoffman, J. P. Omtvedt, G. K. Pang, J. M. Schwantes, S. Soverna, P. Sprunger, R. Sudowe, R. E. Wilson, and H. Nitsche, *Phys. Rev. C* **72**, 14605 (2005).
- (10) K. Morita, K. Morimoto, D. Kaji, T. Akiyama, S. Goto, H. Haba, E. Ideguchi, R. Kanungo, K. Katori, H. Koura, H. Kudo, T. Ohnishi, A. Ozawa, T. Suda, K. Sueki, H. S. Xu, T. Yamaguchi, A. Yoneda, A. Yoshida, and Y. L. Zhao, *J. Phys. Soc. Jpn.* **73**, 2593 (2004).
- (11) G. Giardina, S. Hofmann, A. I. Muminov, and A. K. Nasirov, *Eur. Phys. J. A* **8**, 205 (2000).
- (12) G. G. Adamian, G. Giardina, and A. K. Nasirov, *Proc. XIV Int. Workshop on Nuclear Fission Physics*, Ed. A. Goverdovski, Institute for Physics and Power Engineering, Obninsk (2000), p 106.
- (13) G. Fazio, G. Giardina, A. Lamberto, R. Ruggeri, C. Saccà, R. Palamara, A. I. Muminov, A. K. Nasirov, U. T. Yakhshiev, F. Hanappe, T. Materna, and L. Stuttgé, *J. Phys. Soc. Jpn.* **72**, 2509 (2003).
- (14) G. Fazio, G. Giardina, A. Lamberto, R. Ruggeri, C. Saccà, R. Palamara, A. I. Muminov, A. K. Nasirov, U. T. Yakhshiev, F. Hanappe, T. Materna, and L. Stuttgé, *Eur. Phys. J. A* **19**, 89 (2004).
- (15) G. G. Adamian, R. V. Jolos, A. K. Nasirov, and A. I. Muminov, *Phys. Rev. C* **56**, 373 (1997).
- (16) A. K. Nasirov, A. Fukushima, Y. Toyoshima, Y. Aritomo, A. I. Muminov, Sh. A. Kalandarov, and R. K. Utamuratov, *Nucl. Phys. A* **759**, 342 (2005).
- (17) S. Raman, C. H. Malarkey, W. T. Milner, C. W. Nestor, Jr., and P. H. Stelson, *At. Data Nucl. Data Tables* **36**, 1 (1987).
- (18) R. H. Spear, *At. Data Nucl. Data Tables* **42**, 55 (1989).
- (19) A. D'Arrigo, G. Giardina, M. Herman, A. V. Ignatyuk, and A. Taccone, *J. Phys. G* **20**, 365 (1994).
- (20) R. N. Sagaidak, R. N. Sagaidak, V. I. Chepigin, A. P. Kabachenko, J. Rohác, Yu. Ts. Oganessian, A. G. Popeko, A. V. Yeremin, A. D'Arrigo, G. Fazio, G. Giardina, M. Herman, R. Ruggeri, and R. Sturiale, *J. Phys. G* **24**, 611 (1998).
- (21) G. Fazio, G. Giardina, A. Lamberto, C. Saccà, R. Palamara, A. I. Muminov, A. K. Nasirov, K. V. Pavliy, F. Hanappe, T. Materna, and L. Stuttgé, *J. Phys. Soc. Jpn.* **74**, 307 (2005).
- (22) R. Bock, Y. T. Chu, M. Dakowski, A. Gobbi, E. Grosse, A. Olmi, H. Sann, D. Schwalm, U. Lynen, W. Müller, S. Bjornholm, H. Esbensen, W. Wölfli, and E. Morenzoni, *Nucl. Phys. A* **388**, 334 (1982).

